

Effects of the Electrode Modification Conditions on the Performance of Three-state Electrochromic Devices via Spin-coating

L. Wu, L.X. Fei, D.J. Yang, F. Wu, X.L. Peng, Y.L. Zhu, S.P. Song, Y. Xiang*

School of Energy Science and Engineering, University of Electronic Science and Technology of China, 2006 Xiyuan Ave, West High-Tech Zone, Chengdu, Sichuan 611731, China.

*E-mail: xyg@uestc.edu.cn

Received: 24 May 2017 / *Accepted:* 17 June 2017 / *Published:* 12 July 2017

Electrodeposition-based electrochromic devices capture numerous attentions due to their simple sandwich-type structure, facile and low-cost fabrication, and promising application. Herein, titanium dioxide (TiO₂) nanoparticles were modified onto fluorine doped tin oxide (FTO) electrode via spin-coating technique with different rotation speed and precursor solution concentration, followed by sandwiching a suitable amount of gel electrolyte between the modified FTO electrode and a flat FTO electrode to fabricate the electrodeposition-based electrochromic device with reversible three-state optical transformation (transparent, mirror and black). A systematic study of correlation between electrode modification condition and morphological features of TiO₂ thin films, as well as the performance of electrochromic devices, i.e. optical contrast, switching time, and cycling stability, were investigated. Optimized performances of three-stated electrochromic device could be obtained by properly manipulating the electrode modification conditions. The results in this study will provide valuable guidance for rational design of electrochromic device with satisfactory performance.

Keywords: Electrochromic; Spin-coating; Rotation Speed; Precursor Solution Concentration; Morphological Features; Electrochromic Properties

1. INTRODUCTION

An attractive feature of electrochromic materials is the ability to change their optical properties in a reversible and persistent manner when applied with an electrical voltage. Since the pioneering work of Deb [1], a variety of electrochromic materials have been developed, which can be grouped into several subsets: transition metal oxides [2, 3], Prussianblue [4, 5], conducting polymers [6, 7], viologens [8, 9], transition metal ions coordination compound [10, 11], hybrid electrochromic

materials [12, 13], and reversible electrodeposition-based electrochromic materials [14, 15]. Their electrochromic performances regard to optical contrast, switching time, coloration efficiency, cycling stability, and optical memory effect et al., have been investigated extensively, which promote us to expand the applications of electrochromic materials in the area of smart windows, antiglare rear-view mirrors, electrochromic display, electronic papers, and military camouflage [14-22].

Electrochromic devices based on reversible electrodeposition are promising for application in light modulating devices owing to their simple sandwich-type structure, facile and low-cost fabrication. Their optical properties can be manipulated via deposition of metal (copper, bismuth, plumbum, nickel, silver, etc.) onto transparent conducting electrodes under an applied electrical voltage, and dissolution of metal back into electrolyte upon removal of the voltage [23-33]. Ag-based electrodeposition system [26-33] has been widely developed for fabricating electrochromic devices for its ability to realize mirror state. Araki et al [28] deposited Ag onto an indium tin oxide (ITO) electrode, the surface of which was modified by ITO nanoparticles using spin-coating technique, and obtained an electrochromic device with a reversible three-state optical transformation. In a previous study, our group fabricated an electrodeposition-based Ag/Cu electrochromic device with reversible three-state optical transformation (transparent, black and mirror states), with one of the electrode was modified by TiO₂ nanoparticles via spin-coating technique [31].

The electrochromic properties (i.e. optical contrast, switching time, coloration efficiency, cycling stability, and optical memory effect) of electrochromic materials basically depends on their structural, surface morphological, and compositional, which is mainly controlled by preparation conditions [34]. It is thus extremely necessary to have a closer inspection of preparation parameters for the improvement of electrochromic materials' properties. Deepa et al [35] investigated the influence of varied relative humidity (RH, 55% RH and 75% RH) during dip-coating tungsten oxide (WO₃) thin film from an oxalato-acetylated peroxotungstic acid sol on the microstructure and electrochromic properties of WO₃ films. Sun and co-workers [36] investigated the influence of annealing temperature on the microstructure and optical properties of WO₃ films prepared by sol-gel route combined with spin-coating method. The effects of the type and content of organic moiety in the precursor sol, film preparation method (spin or dip coating) on film properties have also been investigated extensively [36, 37], to have a general understanding of correlation between the electrochromic performance and the fabrication parameters of electrochromic thin films. Tsuboi and co-workers [29, 30] demonstrated that multiple colour states of electrochromic device can be controlled by manipulating the size and shape of of Ag grains under different voltages. Xiang et al [31]. investigated the influence of nanoparticle size on microstructure of TiO₂ films prepared by spin-coating method and optical properties of fabricated reversible three-state device. The results illustrated that the optical properties of the device in different states can be controlled effectively by manipulating the surface structure of the TiO₂ modified FTO electrode. To the best of our knowledge, the closer inspection of effects of electrode surface modification on the electrochromic device with multiple states are, however, rarely reported. Therefore, a thorough investigation on electrodeposition-based electrochromic devices properties through the fabrication parameters is of scientific importance.

In this study, TiO₂ nanoparticles were modified onto FTO via spin-coating technique, followed by sandwiching a suitable amount of gel electrolyte between a modified FTO electrode and a flat FTO

electrode to fabricate electrodeposition-based electrochromic device. Under a suitable voltage, the fabricated electrochromic device changes its optical states from transparent to mirror or black state depending on whether the silver deposit on the flat FTO electrode or the opposite rough FTO electrode modified using TiO₂ nanoparticles. Reversely, Ag is dissolved into the gel electrolyte once the voltage is removed and the device changes back to transparent state. The precursor solution concentration is an important parameter that can be manipulated and could make the performance of fabricated devices different. Therefore, the precursor solution concentration was adjusted to investigate its effects on the microstructures of TiO₂ thin films and performance of fabricated devices. Except for the precursor solution concentration, the rotation speed is the main parameter during the spin-coating processes. Herein, the rotation speed was also varied to investigate their effects on the microstructure of TiO₂ thin films as well as the performance of electrochromic devices, i.e. transmittance/reflectance, optical contrast, switching time, and cycling stability. The results in this study will provide valuable guidance for rational design of electrochromic device with satisfactory performance.

2. EXPERIMENTAL

2.1 Materials

FTO transparent conducting glasses with the size of 25×30 mm, the thickness of 2.2 mm, and a sheet resistance of 10 Ω sq⁻¹ were used as the electrodes, which were purchased from Wuhan Lattice Solar Energy Technology Co. Ltd. Uniform TiO₂ nanoparticles with average diameter of 5~10 nm (Aladdin Co. Ltd) were used to modify the FTO electrodes. Electrolytes compounds including Dimethyl sulfoxide (DMSO, ≥99.8%, J&K Chemical Co. Ltd.), tetra-n-butylammoniumbromide (TBABr, ≥99%, J&K Chemical Co. Ltd.), silver nitrate (AgNO₃, ≥99.8%, Guangdong Guanghua Sci-Tech Co. Ltd.), copper chloride (CuCl₂, ≥99.0%, KeLong Chemical Co. Ltd.), poly (vinyl butyral) (PVB, Sekisui Chemical Co. Ltd.), ethyl cellulose (≥99.5%, Hanzhou Lanbo Industrial Co. Ltd.), lauric acid (≥99.8%, KeLong Chemical Co. Ltd.), terpineol (≥98.0%, KeLong Chemical Co. Ltd.) and ethyl alcohol (≥99.7%, KeLong Chemical Co. Ltd.) were obtained from commercial sources. All solvents and chemicals were of reagent quality and were used without further purification. Teflon sheets (Aladdin Co. Ltd) with a thickness of 0.5 mm were cut into 25 × 25 mm with a 20 × 20 mm hole. Both FTO glass electrodes and Teflon sheets were cleaned with ethanol and de-ionized water several times before use.

2.2 Preparation of TiO₂ nanoparticles dispersion and gel electrolyte

To prepare the TiO₂ nanoparticle dispersion, TiO₂ nanoparticles (raw materials, 2.5 g) with lauric acid (surfactant, 0.25 g) and ethyl cellulose (adhesive, 0.75 g) were placed into a ball-mill jar at first, mixed with terpineol (adhesive, 16 mL) and ethyl alcohol (solvent, 10 mL) immediately before milling. TiO₂ nanoparticle slurry was obtained after 50 min milling, followed by diluting the slurry with ethyl alcohol. To prepare the gel electrolyte, TBABr (806 mg, 2.5 mmol), silver nitrate (85 mg,

0.5 mmol), and copper chloride (13 mg, 0.1 mmol) were dissolved in 10 mL of DMSO, followed by the addition of PVB (1.32 g, 10 wt%). Finally, the mixed solution was placed in the dark for 24–48 hours to obtain the gel electrolyte.

2.3 Modification of FTO electrode and fabrication of electrochromic devices

The ethyl alcohol (10 mL, 15 mL, or 20 mL) as a diluent was added to TiO₂ nanoparticle dispersion (5 mL), ultrasonically mixed for 30 min. Subsequently, the FTO electrode with tape pasted on the upper front was fixed on the spin-coater, the surface of the FTO electrode was added with 0.25 mL of the above mentioned dispersion, and rotated with two different speeds: a speed of 500 rpm for 5 s, followed by a given speed for the next 15 s. The TiO₂ nanoparticle-modified FTO conducting electrode was obtained by sintering the as-prepared samples for 30 min at 500 °C. For comparison, different rotation speeds (1000 rpm, 2000 rpm, and 3000 rpm) and precursor solution concentrations (ratio of TiO₂ nanoparticle dispersion and ethyl alcohol of 1:2, 1:3, and 1:4) were used in this study. Specifically, to investigate the effects of rotation speed on the performance of electrochromic device, rotation speed of 1000 rpm, 2000 rpm, and 3000 rpm were used by fixing the TiO₂ nanoparticles size of 5–10 nm and the precursor concentration to be 1:2. To investigate the effects of precursor concentration on the performance of electrochromic device, ratio of TiO₂ nanoparticle dispersion and ethyl alcohol of 1:2, 1:3, and 1:4 were used by fixing the TiO₂ nanoparticles size of 5–10 nm and the rotation speed of 2000 rpm. To assemble the electrodeposition-based electrochromic device, the DMSO-based gel electrolyte was contained in a hermetic square space of 20 mm × 20 mm, cut inside a Teflon sheet of 0.5 mm thickness, and sealed by sandwiching the Teflon sheet between two FTO electrodes, one of which was modified with TiO₂ nanoparticles.

2.4 Characterization

The morphology of TiO₂ nanoparticles modified FTO electrodes were characterized using a field-emission scanning electron microscope (FE-SEM, S-3400, Hitachi). The roughness of TiO₂ nanoparticles modified FTO electrodes were characterized by using an atomic force microscope (AFM, Multimode V, Veeco). The electrochemical CV tests were conducted by using an electrochemical workstation (CHI660D, CHI), with the negative pole and positive pole of a power source connected to the flat FTO electrode and TiO₂ nanoparticle-modified FTO electrode respectively. The counter electrode of the electrochromic device during the measurement was the flat FTO electrode and the working electrode was the TiO₂ nanoparticle-modified FTO electrode. The transformation voltage was applied to the electrochromic devices using the electrochemical workstation (CHI660D, CHI), and the transmittance and reflectance spectra were measured using a UV-Vis spectrophotometer (Cary 5000, Agilent). All the electrochromic properties including optical contrast, switching time, and cycling stability were obtained by using a two-electrode mode. Specifically, to characterize the optical contrast, voltages of +2.5 V and -2.5 V were applied to the TiO₂ nanoparticle-modified FTO electrode for 20 s to measure the

transmittance and reflectance spectra of the devices with transparent, black, and mirror states in the spectrum range of 400 nm ~ 800 nm. To characterize the switching time, time-dependent transmittance changes of the devices at 700 nm were measured during 2-electrode CV tests, with voltages of +2.5 V and -2.5 V alternately applied to the TiO₂-modified FTO electrodes for 20 s, and with four consecutive coloration/bleaching cycles and a sweep rate of 100 mV/s. To characterize the cycling stability, transmittance of devices in the transparent and black states were measured every 500 cycles via the UV-Vis spectrophotometer after applying a sequence of voltages in the order of -2.5 V (10 s), 0.5 V (30 s), 2.5 V (10 s), 0.5 V (20 s).

3. RESULTS AND DISCUSSION

3.1 Realizing reversible three-state optical transformation for voltage-controlled electrochromic device

Basically, reversible three-state optical transformation among mirror, black and transparent states can be achieved by alternately applying/removing suitable voltages on the electrodeposition-based electrochromic device. The black and mirror states would be triggered by Ag deposition on the rough TiO₂ nanoparticle-modified FTO electrode and on the flat electrode, respectively. Accordingly, the black state of the modified device can be strongly influenced by their surface morphological structures [29-31].

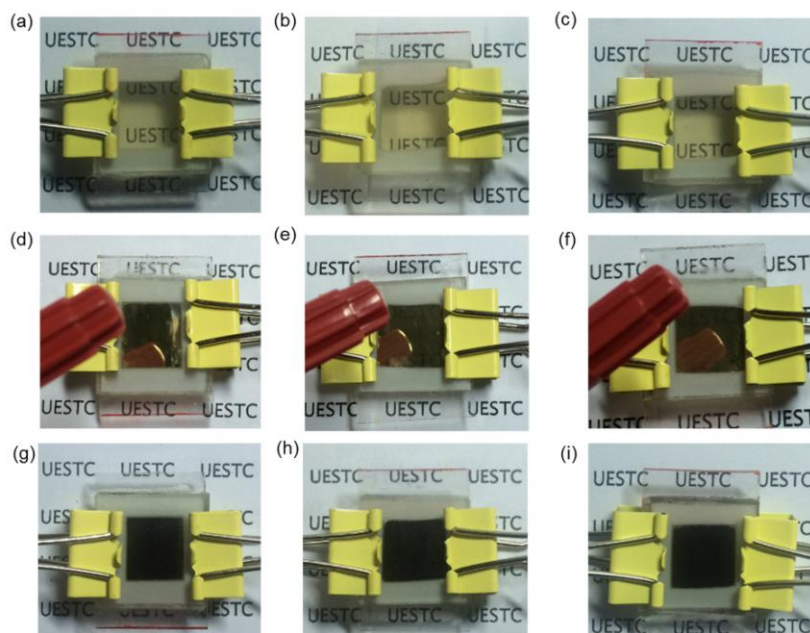


Figure 1. Photographs of the electrodeposition-based electrochromic device prepared with rotation speed of 1000 rpm in (a) transparent state, (d) mirror state, and (g) black state; Photographs of the electrodeposition-based electrochromic device prepared with rotation speed of 2000 rpm in (b) transparent state, (e) mirror state, and (h) black state; Photographs of the electrodeposition-based electrochromic device prepared with rotation speed of 3000 rpm in (c) transparent state, (f) mirror state, and (i) black state.

To investigate the effects of the surface morphological structure of the TiO_2 thin film on the performance of the modified devices, TiO_2 thin films prepared with rotation speed of 1000 rpm, 2000 rpm, and 3000 rpm were fabricated, followed by sintering treatments, and sandwiching a suitable amount of gel electrolyte between the modified FTO electrodes and the flat FTO electrodes. By applying suitable voltages, the electrochromic devices prepared with different rotation speed exhibit three reversible optical states, including transparent, mirror, and black, as illustrated in Figure 1. The essential mechanism of the transformed optical states is Ag deposition onto transparent conducting electrodes and dissolution into the electrolyte according to previous reports [27-32, 38-40]. Without applying voltage, the device is transparent, as the background letters UESTC can be seen clearly (Figure 1a, 1b, and 1c). When a positive voltage (+2.5 V) is applied to the modified FTO electrode, the device turns into the mirror state, with the deposition of Ag onto the unmodified FTO electrode (flat surface), as proved by the reflection image of the red pen in Figure 1d, 1e and 1f. Similarly, the black state is obtained by applying a negative voltage (-2.5 V) to the modified FTO electrode (rough surface), as shown in Figure 1g, 1h and 1i. Thus it can be seen that the spin-coated electrodeposition-based electrochromic devices prepared with different rotation speed can all realize the voltage controlled three-state optical transformation among transparent, mirror, and black states.

3.2 Morphological features of the spin coated TiO_2 thin films prepared with different rotation speed

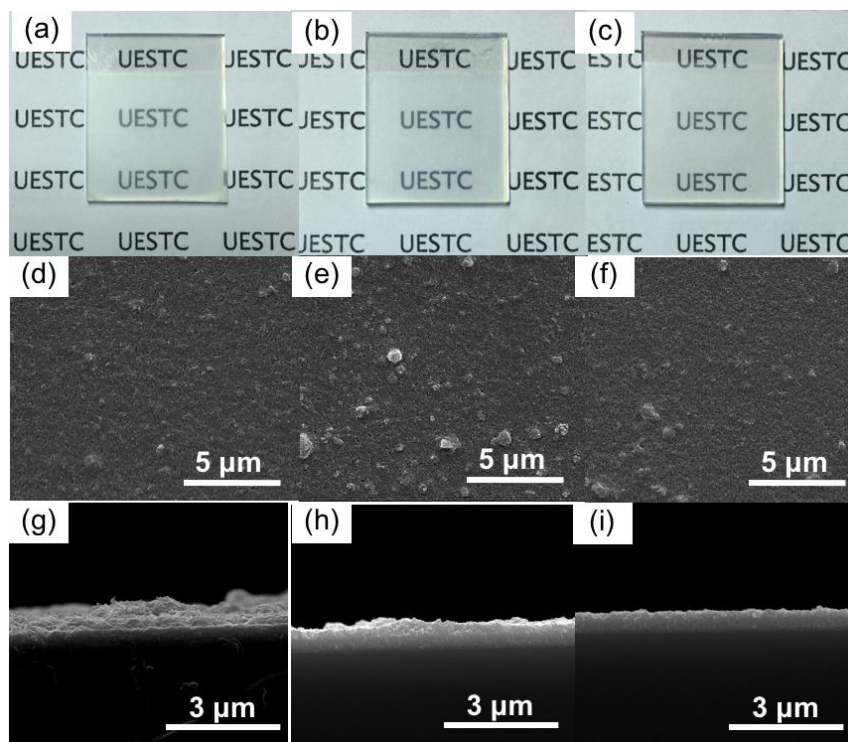


Figure 2. Photographs of TiO_2 thin films prepared with rotation speed of (a) 1000 rpm, (b) 2000 rpm, and (c) 3000 rpm, respectively. In-plane SEM images of TiO_2 thin films prepared with rotation speed of (d) 1000 rpm, (e) 2000 rpm, and (f) 3000 rpm, respectively. Cross-sectional SEM images of TiO_2 thin films prepared with rotation of (g) 1000 rpm, (h) 2000 rpm, and (i) 3000 rpm, respectively.

The morphological features of the three spin-coated TiO₂ thin films prepared with rotation speed of 1000 rpm, 2000 rpm, and 3000 rpm were investigated. Photographs, in-plane and cross-sectional SEM images of the spin-coated TiO₂ thin films are provided in Figure 2. The FTO electrodes coated with TiO₂ thin films spin-coated with different rotation speed show different transparency and gradually blurred after decreasing the rotation speed to 1000 rpm (Figure 2a, 2b, and 2c). Since the thickness of the spin-coated thin film is dependence on the rotation speed [41], the gradually blurred modified FTO electrodes surface may be due to the increase in the TiO₂ thin film thickness for the lower rotation speed. The SEM micrographs of the spin-coated TiO₂ thin films prepared with different rotation speed are displayed in Figure 2d, 2e and 2f. The spin-coated TiO₂ thin films prepared with different rotation speed exhibit difference in inhomogeneous distribution of TiO₂ nanoparticles in terms of slightly decreased nanoparticles agglomeration observed for the TiO₂ thin film prepared with lower rotation speed (Figure 2d, 2e, and 2f). As shown in Figure 2d, 2e, and 2f, all the three TiO₂ thin films present sharp and well-defined boundaries between grains as well as different sized pores inside, indicating a fine-grained TiO₂ thin film obtained. The cross-sectional SEM images of TiO₂ thin films prepared with rotation speed of 1000 rpm, 2000 rpm, and 3000 rpm are presented in Figure 2g, 2h and 2i. Typically, a decrease in thickness of the three TiO₂ thin films with higher rotation speed are measured through the cross-sectional SEM images, with the thickness of TiO₂ thin film of 420 nm, 320 nm, and 130 nm for FTO electrodes prepared with rotation speed of 1000 rpm, 2000 rpm, and 3000 rpm observed, respectively. In addition, rough and loose surface with dozens of nanoparticles distributed is observed for TiO₂ thin film prepared with lower rotation speed (Figure 2g), indicating the influence of rotation speed on the morphological features of spin-coated TiO₂ thin film.

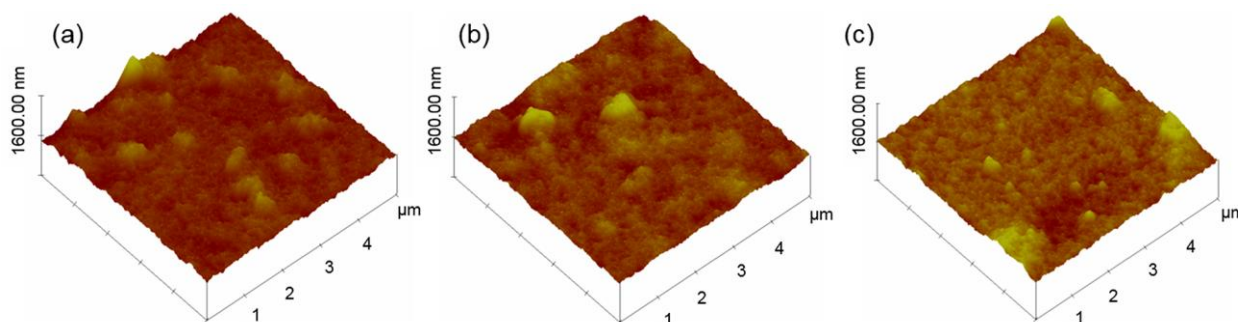


Figure 3. AFM image of spin-coated TiO₂ thin film with rotation speed of (a) 1000 rpm, (b) 2000 rpm, and (c) 3000 rpm, respectively.

The surface roughness of the spin-coated TiO₂ thin films prepared with different rotation speed were further measured by using an atomic force microscope (AFM), as shown in Figure 3a, 3b and 3c. Rough surface with different distributed bumps and holes are exhibited for the TiO₂ thin films prepared with rotation speed of 1000 rpm, 2000 rpm, and 3000 rpm [42]. Surface average roughness of 59 nm (5 $\mu\text{m}\times 5\ \mu\text{m}$), 50 nm (5 $\mu\text{m}\times 5\ \mu\text{m}$), and 51 nm (5 $\mu\text{m}\times 5\ \mu\text{m}$) are measured for the TiO₂ thin films prepared with rotation speed of 1000 rpm, 2000 rpm, and 3000 rpm. The

varied surface roughness for TiO₂ thin films prepared with different rotation speed indicates that the rotation speed is crucial for the surface morphology of the spin-coated TiO₂ thin film, which is an important factor for the electrochromic properties such as switching speed and cycling stability, etc.

3.3 Investigation on the optical properties of spin-coated electrochromic device prepared with different rotation speed

To further investigate the influence of rotation speed on the performance of electrochromic device, transmittance and reflectance spectra of the spin-coated devices prepared with rotation speed of 1000 rpm, 2000 rpm, and 3000 rpm were measured in the spectrum range of 400 nm~800 nm. For transmittance and reflectance measurement, voltages of +2.5 V and -2.5 V are applied to the TiO₂ nanoparticle-modified FTO electrode to obtain the mirror and black states, respectively. As shown in Figure 4a, 4b, and 4c, increased transmittance for devices in transparent state with the increase of rotation speed is measured, with the transmittance of 52%, 61%, and 64% at 700 nm obtained, respectively.

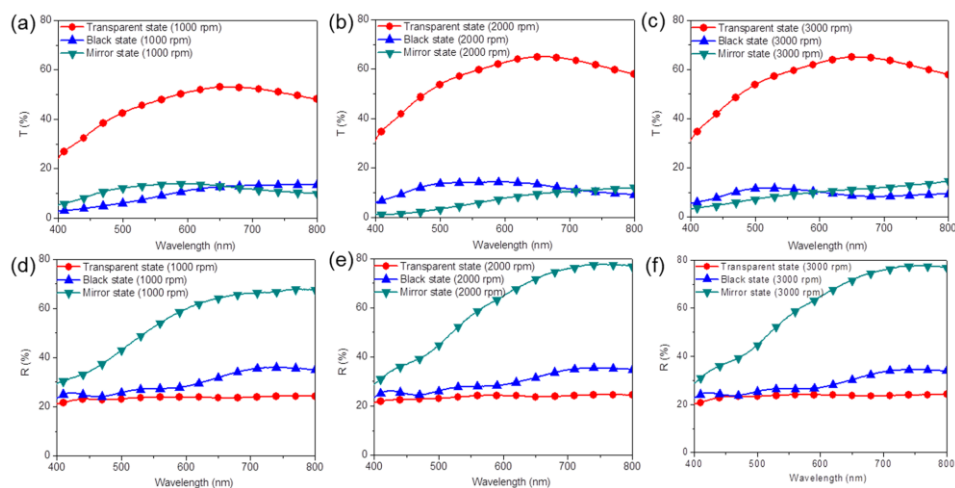


Figure 4. Transmittance spectra of devices in transparent (red), black (blue), and mirror states (green), prepared with rotation speed of (a) 1000 rpm, (b) 2000 rpm, and (c) 3000 rpm; Reflectance spectra of devices in transparent (red), black (blue), and mirror states (green), prepared with rotation speed of (d) 1000 rpm, (e) 2000 rpm, and (f) 3000 rpm.

The increased transmittance in transparent is obtained for modified device prepared with rotation speed of 3000 rpm thanks to the lowest thickness of spin-coated thin film, as illustrated in Figure 2. When applied with a negative voltage, the Ag is deposited onto the modified FTO electrode, leading to the device changes its optical state from transparent to black state, the transmittance drops to 13%, 9%, and 8% at 700 nm quickly. The low transmittance appears to be comparable to the cell transmittance observed for ITO nanoparticles spin-coated device in coloration states [28]. The optical contrast, which is defined as the maximal difference of transmittance for electrochromic device between its coloration and bleaching processes, are measured to be 39%, 52%,

and 56%, which is as high as that reported by He et. al [43]. After trigger the mirror state by applying a positive voltage, decrease in transmittance for device is also observed [39, 40, 43], as illustrated in Figure 4a, 4b, and 4c. The reflectance spectra for devices prepared with rotation speed of 1000 rpm, 2000 rpm, and 3000 rpm are also measured. As shown in Figure 3d, 3e, and 3f, the reflectance for devices in transparent and black states prepared with rotation speed of 1000 rpm, 2000 rpm, and 3000 rpm are all measured approximate 24% and 34%, respectively. The devices in mirror state exhibits reflectance over 70%, as expected (Figure 4d, 4e, and 4f). The obtained high reflectance is in good agreement with literature data [44].

3.4 Study of response speed and cycling stability of the spin-coated devices prepared with different rotation speed

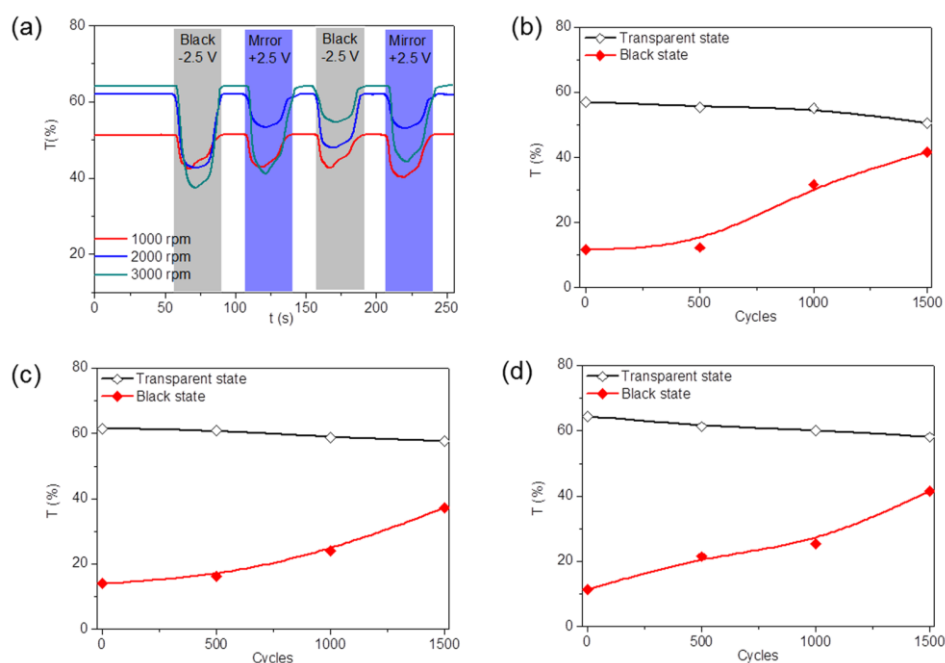


Figure 5. Transmittance variations at 700 nm obtained during 2-electrode CV tests for devices modified with rotation speed of 1000 rpm (red), 2000 rpm (blue), and 3000 rpm (green), respectively (a); transmittance variation for spin-coated device prepared with rotation speed of (b) 1000 rpm, (c) 2000 rpm, and (d) 3000 rpm, in transparent (black) and black (red) states at 700 nm after applying a sequence of voltages in the following order: -2.5 V (10 s), 0.5 V (30 s), 2.5 V (10 s), 0.5 V (20 s), with each of the 500 cycles was taken as a measurement node.

Time-dependent transmittance changes of the three modified devices at 700 nm were measured during 2-electrode CV tests, with four consecutive coloration/bleaching cycles and a sweep rate of 100 mV/s. For transmittance measurement, voltages of +2.5 V and -2.5 V were alternately applied to the TiO₂-modified FTO electrodes for 20 seconds. Figure 5a shows the transmittance variation over time for modified devices prepared with rotation speed of 1000 rpm, 2000 rpm, and 3000 rpm. The initial transmittance of the modified devices prepared with rotation speed of 1000 rpm, 2000 rpm, and 3000 rpm attain 52%, 61%, and 64% upon bleaching and drops to 42%, 40%, 37%

upon coloration, respectively. Basically, Coloration-bleaching switching time is expressed as the time needed to reach 90% of its maximum modulation during coloration and bleaching processes, which is strongly determined by the morphology of the film [45]. The coloration time of modified device prepared with rotation speed of 1000 rpm, 2000 rpm, and 3000 rpm are measured to be 6.7 s, 7.5 s, and 6.8 s, respectively. The bleaching time of these modified devices are measured to be 19.4 s, 16.4 s, and 18.9 s, illustrating that an FTO electrode modified with smoother TiO₂ thin film contributes to the shorter bleaching switching time. The influence of rotation speed on the bleaching time of electrochromic device might be due to the varied TiO₂ thin film surface morphological features. Generally, in comparison with compact thin films, the rough thin films offer potential advantages in the electrochromic device due to their large active surface area that could increase the efficient contact area between the electrode and the electrolyte [46]. Although, the larger active surface area of TiO₂ thin film obtained by spin-coating has the ability to accelerate the Ag deposition onto FTO electrode, the Ag dissolution back into electrolyte is, however, slowed down. Accordingly, the rougher surface with more nanoparticles agglomeration will hinder the dissolution Ag back into the gel electrolyte, which prolongs the bleaching time from coloration to transparent state. Furthermore, the bleaching process is slower than coloration process for all devices, which is illustrated by most articles about electrochromic devices [31, 47].

Furthermore, when an electrochromic device is repeatedly switched between its coloration and bleached states for a certain number of times, device failure occurs due to various faults and side reactions, such as electrode failure, electrolyte deprivation, decay of active layer etc. Generally, the cycling stability can be characterized by measuring the optical contrast after repeatedly applying sequential voltages [28, 31, 48]. To investigate the cycling stability of modified devices prepared with rotation speed of 1000 rpm, 2000 rpm, and 3000 rpm, transmittance at 700 nm of spin-coated device in the transparent and black states was measured every 500 cycles by applying voltages of -2.5 V, via the UV-Vis spectrophotometer. As shown in Figure 5b, 5c, and 5d, the transmittance in transparent state is decreased and the transmittance in black state is slightly increased with the increase of cycles, with more cycles leading to poorer stability, as reported by previous literatures [28, 31, 48]. After 1500 cycles, the optical contrast of modified devices prepared with rotation speed of 1000 rpm, 2000 rpm, and 3000 rpm drops from 45%, 51%, 53% to 9%, 21%, and 17%, indicates that the change in optical transmittance contrast are measured to be 80%, 60%, and 68%. It is thus can be seen that the smallest change in optical transmittance contrast is observed for the device prepared with rotation speed of 2000 rpm. We suppose that the ability to achieve complete reversibility is deteriorated due to the gradual deposition of Ag onto bumps of TiO₂ thin films and inability to dissolve Ag back into electrolyte immediately during the continuous cycling between the coloration and bleaching states. For the modified device prepared with rotation speed of 3000 rpm, the higher change in optical transmittance contrast than that of the device prepared with rotation speed of 2000 rpm might be due to the discontinuous TiO₂ thin films as a result of its low thickness. The comparative study of spin-coated TiO₂ thin films prepared with different rotation speed reveals that the electrochromic properties can be strongly influenced by the film preparation parameters as aforementioned.

3.5 Investigation on the performance of spin-coated electrochromic device prepared with different precursor solution concentration

As aforementioned, the performance of the corresponding electrochromic device is varied for spin-coated TiO₂ thin film prepared with different rotation speed, indicating the strong influence of the modification parameters on the morphological features of TiO₂ thin film and the performance of the corresponding electrochromic device. Except for the rotation speed, the precursor solution concentration is also an important parameter that can be manipulated and could make the performance of fabricated devices different. Therefore, the precursor solution concentration was subsequently adjusted to investigate its effects on the morphological features of TiO₂ thin films and performance of fabricated devices. Specifically, ratio of TiO₂ nanoparticle dispersion and ethyl alcohol of 1:2, 1:3, and 1:4 were prepared, followed by spin-coating on FTO electrodes with rotation speed of 2000 rpm, sintering treatment for 30 min at 500°C, and assembling as “sandwich-type” structured electrodeposition-based electrochromic device. Firstly, the transmittance and reflectance spectra of the spin-coated devices prepared with ratio of TiO₂ nanoparticle dispersion and ethyl alcohol of 1:2, 1:3, and 1:4 were measured in the spectrum range of 400 nm~800 nm. The optical contrast of modified devices prepared with ratio of TiO₂ nanoparticle dispersion and ethyl alcohol of 1:2, 1:3, and 1:4 are measured to be 52%, 58%, and 59% (Figure 6a, 6b, and 6c). As illustrated above, the increased optical contrast with the decreased of precursor solution concentration is the result of the decreased thickness of TiO₂ thin film [49]. The reflectance (mirror state) approximate 80% were also obtained for the modified devices prepared with ratio of TiO₂ nanoparticle dispersion and ethyl alcohol of 1:2, 1:3, and 1:4 (Figure 6d, 6e, and 6f). Similarly, sharply reduced reflectance is observed for devices prepared with different precursor solution concentration in transparent and black states.

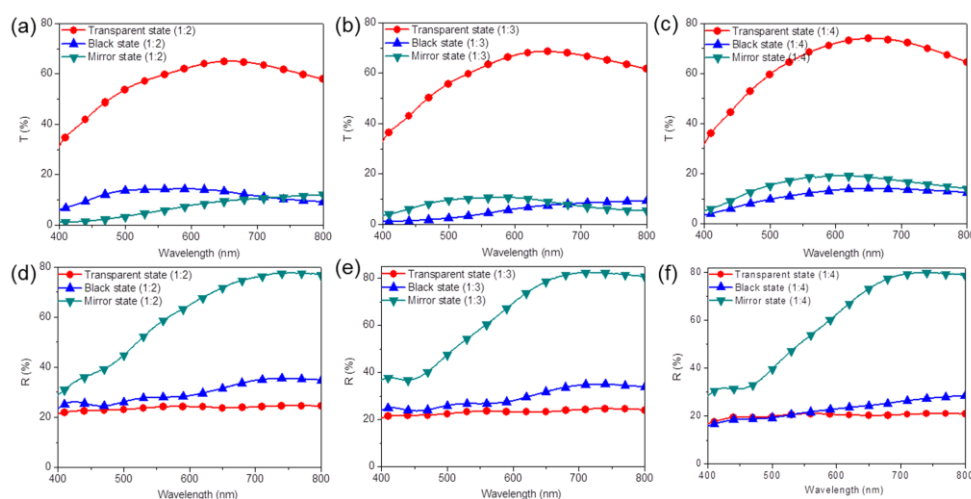


Figure 6. Transmittance spectra of devices in transparent (red), black (blue), and mirror states (green) prepared with ratio of TiO₂ nanoparticle dispersion and ethyl alcohol of (a) 1:2, (b) 1:3; (c) 1:4; reflectance spectra of devices in transparent (red), black (blue), and mirror states (green) prepared with ratio of TiO₂ nanoparticle dispersion and ethyl alcohol of (d) 1:2, (e) 1:3, (f) 1:4.

Figure 7a shows the transmittance variation over time for modified devices prepared with ratio of TiO₂ nanoparticle dispersion and ethyl alcohol of 1:2, 1:3, and 1:4. The initial transmittance of the modified devices prepared with precursor solution concentration of 1:2, 1:3, and 1:4 attain 61%, 67%, and 69% upon bleaching and drops to 40%, 57%, 51% upon coloration, respectively. The coloration speed is slowed down to 9 s and the bleaching time is speeded up to 16.2 s by decreasing the precursor solution concentration to 1:4. The transmittance at 700 nm of modified devices prepared with different precursor solution concentration in the transparent and black states were shown in Figure 7b, 7c, and 7d. The change in optical transmittance contrast after 1500 cycles are measured to be 60%, 50%, and 53% for modified devices prepared with precursor solution concentration of 1:2, 1:3, and 1:4, indicating improved cycling stability of electrochromic device prepared with lower precursor solution concentration.

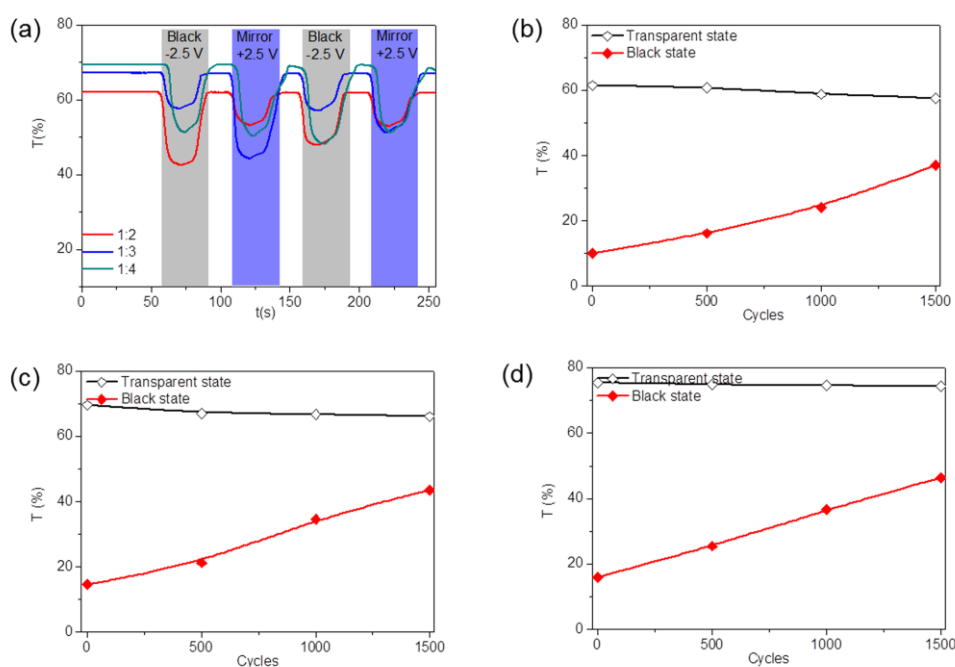


Figure 7. Transmittance variations at 700 nm obtained during 2-electrode CV tests for devices modified with precursor solution concentration of 1:2 (red), 1:3 (blue), and 1:4 (green), respectively (a); transmittance variation for spin-coated device prepared with precursor solution concentration of (b) 1:2, (c) 1:3, and (d) 1:4, in transparent (black) and black (red) states at 700 nm after applying a sequence of voltages in the following order: -2.5 V (10 s), 0.5 V (30 s), 2.5 V (10 s), 0.5 V (20 s), with each of the 500 cycles was taken as a measurement node.

The electrochromic properties, including optical contrast, switching speed, and cycling stability are related to the morphological features of the TiO₂ thin film prepared with different modification conditions [34]. The morphological features of the spin-coated TiO₂ thin films prepared with different precursor solution concentrations were investigated by SEM and AFM. As shown in Figure 8a, 8b, and 8c, less nanoparticles agglomeration is observed for the TiO₂ thin film prepared with precursor solution concentration of 1:4 (Figure 8c). The thickness of the TiO₂ thin films exhibits decreased

tendency with the decrease of precursor solution concentration as expected [49], with 320 nm, 153 nm, and 95 nm obtained for TiO₂ thin films prepared with precursor solution concentration of 1:2, 1:3, and 1:4 (Figure 8d, 8e, and 8f). This decreased thickness is resulted in the increased optical contrast, as illustrated in Figure 5a, 5b, and 5c. The surface of TiO₂ thin films prepared with different precursor solution concentration exhibits different distributed bumps and holes, indicates that rough layers with different roughness are constructed by spin-coating TiO₂ nanoparticles on the FTO electrodes with different precursor solution concentration [50]. Decreased surface average roughness are measured for the TiO₂ thin films prepared with higher precursor solution concentration (Figure 8g, 8h, and 8i). This varied roughness of the TiO₂ thin films prepared with different precursor solution concentration results to the varied switching time and cycling stability, as illustrated in Figure 7.

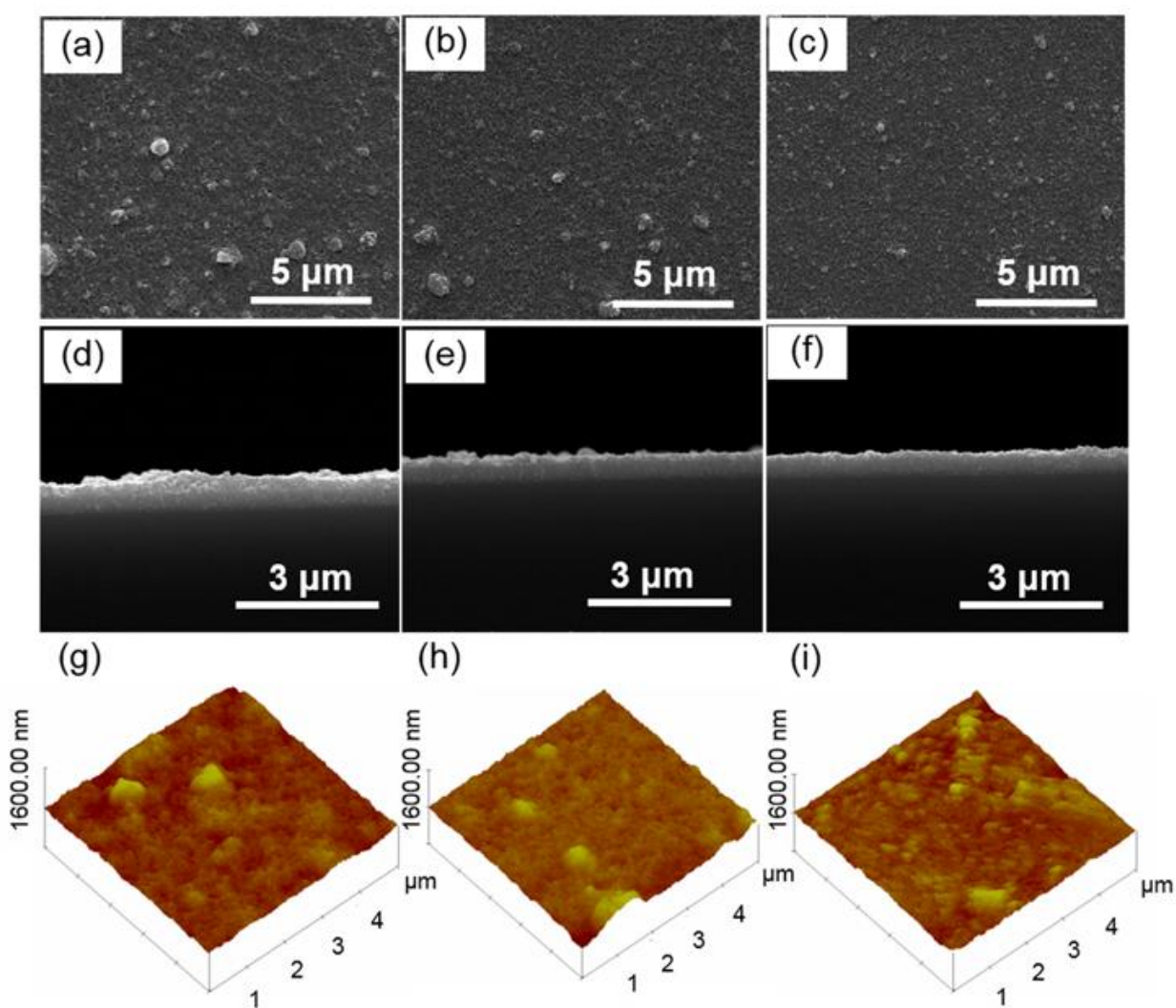


Figure 8. In-plane SEM images of TiO₂ thin films prepared with precursor solution concentration of (a) 1:2, (b) 1:3, and (c) 1:4, respectively. Cross-sectional SEM images of TiO₂ thin films prepared with precursor solution concentration of (d) 1:2, (e) 1:3, and (f) 1:4, respectively. AFM image of spin-coated TiO₂ thin film with precursor solution concentration of (g) 1:2, (h) 1:3, and (i) 1:4, respectively.

4. CONCLUSIONS

In summary, the correlation between the electrode modification parameters, including rotation speed and precursor solution concentration, and the morphological features of the TiO₂ nanoparticle-modified FTO electrodes as well as the optical behavior of the fabricated devices is systematically studied, which reveals that the performance of the three-state electrochromic device can be adjusted by simply manipulating the rotation speed and precursor solution concentration. The optical contrast of the modified electrochromic device is increased with the decreased thickness of TiO₂ thin film, which can be manipulated by using higher rotation speed and lower precursor solution concentration. The switching time of the modified device is strongly influenced by the surface roughness of the spin-coated TiO₂ thin film, with rougher surface providing large active surface area to slow down the bleaching time of the device. The increased nanoparticles agglomeration onto the surface of modified FTO electrode with the decrease in rotation speed and precursor solution concentration will hinder the Ag leave the rough surface easily, leading to a poor cycling stability of the electrodeposition-based electrochromic device. The obstructed Ag dissolution caused by large active surface area is also proved by the longer switching time for device transforms from coloration to transparent state. The results in this study will provide valuable guidance for rational design of electrochromic device with satisfactory performance and the TiO₂ nanoparticle-modified device with reversible three-state optical transformation may have various applications, such as information displays and light-modulation devices.

ACKNOWLEDGEMENTS

The authors acknowledge the financial support from National Natural Science Foundation of China [Grant #: 51472044].

References

1. S. K. Deb, *Appl. Optics*, 8 (1969) 192.
2. B. T. Sone, S. N. Mailu, T. Malwela, E. Coetsee, H. C. Swart, E. I. Iwuoha and M. Maaza, *Int. J. Electrochem. Sc.*, 9 (2014) 2867.
3. G. A. Niklasson and C. G. Granqvist, *J. Mater. Chem.*, 17 (2007) 127.
4. D. M. DeLongchamp and P. T. Hammond, *Adv. Funct. Mater.*, 14 (2004) 224.
5. K. Itaya, I. Uchida and V. D. Neff, *Acc. Chem. Res.*, 19 (1986) 162.
6. K. Lin, S. Zhang, H. Liu, Y. Zhao, Z. Wang and J. Xu, *Int. J. Electrochem. Sc.*, 10 (2015) 7720.
7. W. Lu, A. G. Fadeev, B. H. Qi, E. Smela, B. R. Mattes, J. Ding, G. M. Spinks, J. Mazurkiewicz, D. Z. Zhou, G. G. Wallace, D. R. MacFarlane, S. A. Forsyth and M. Forsyth, *Science*, 297 (2002) 983.
8. T. Kakibe and H. Ohno, *J. Mater. Chem.*, 19 (2009) 4960.
9. X. W. Sun and J. X. Wang, *Nano Lett.*, 8 (2008) 1884.
10. G. de la Torre, C. G. Claessens and T. Torres, *Chem. Commun.*, (2007) 2000.
11. Q. Zeng, A. McNally, T. E. Keyes and R. J. Forster, *Electrochem. Commun.*, 10 (2008) 466.
12. H. Ling, J. Lu, S. Phua, H. Liu, L. Liu, Y. Huang, D. Mandler, P. S. Lee and X. Lu, *J. Mater. Chem. A.*, 2 (2014) 2708.

13. S. Xiong, S. L. Phua, B. S. Dunn, J. Ma and X. Lu, *Chem. Mater.*, 22 (2010) 255.
14. J. P. Ziegler and B. M. Howard, *Sol. Energ. Mat. Sol. C.*, 39 (1995) 317.
15. J. P. Ziegler, *Sol. Energ. Mat. Sol. C.*, 56 (1999) 477.
16. C. Bechinger, S. Ferrer, A. Zaban, J. Sprague and B. A. Gregg, *Nature*, 383 (1996) 608.
17. A. Kraft and M. Rottmann, *Sol. Energ. Mat. Sol. C.*, 93 (2009) 2088.
18. U. Bach, D. Corr, D. Lupo, F. Pichot and M. Ryan, *Adv. Mater.*, 14 (2002) 845.
19. S. I. Cho, W. J. Kwon, S. J. Choi, P. Kim, S. A. Park, J. Kim, S. J. Son, R. Xiao, S. H. Kim and S. B. Lee, *Adv. Mater.*, 17 (2005) 171.
20. F. C. Krebs, *Nature Mater.*, 7 (2008) 766.
21. P. M. S. Monk, C. Turner and S. P. Akhtar, *Electrochim. Acta*, 44 (1999) 4817.
22. M. P. Browne, H. Nolan, N. C. Berner, G. S. Duesberg, P. E. Colavita and M. E. G. Lyons, *Int. J. Electrochem. Sc.*, 11 (2016) 6636.
23. S. I. C. deTorres and I. A. Carlos, *J. Electroanal. Chem.*, 414 (1996) 11.
24. A. Imamura, M. Kimura, T. Kon, S. Sunohara and N. Kobayashi, *Sol. Energ. Mat. Sol. C.*, 93 (2009) 2079.
25. M. Nakashima, T. Ebine, M. Shishikura, K. Hoshino, K. Kawai and K. Hatsusaka, *ACS Appl. Mater. Interfaces*, 2 (2010) 1471.
26. I. Krastev, T. Valkova and A. Zielonka A, *J. Appl. Electrochem.*, 33 (2003) 1199.
27. C. Park, S. Seo, H. Shin, B. D. Sarwade, J. Na and E. Kim, *Chem. Sci.*, 6 (2015) 596.
28. S. Araki, K. Nakamura, K. Kobayashi, A. Tsuboi and N. Kobayashi, *Adv. Mater.*, 24 (2012) OP122.
29. A. Tsuboi, K. Nakamura and N. Kobayashi, *J. Soc. Inf. Display*, 21 (2013) 361.
30. A. Tsuboi, K. Nakamura and N. Kobayashi, *Adv. Mater.*, 25 (2013) 3197.
31. T. Ye, Y. Xiang, H. Ji, C. Hu and G. Wu, *RSC Adv.*, 6 (2016) 30769.
32. C. O. Avellaneda, M. A. Napolitano, E. K. Kaibara and L. O. S. Bulhoes, *Electrochim. Acta*, 50 (2005) 1317.
33. M. R. S. Oliveira, D. A. A. Mello, E. A. Ponzio and S. C. de Oliveira, *Electrochim. Acta*, 55 (2010) 3756.
34. M. Deepa, P. Singh, S. N. Sharma and S. A. Agnihotry, *Sol. Energ. Mat. Sol. C.*, 90 (2006) 2665.
35. X. Sun, H. Cao, Z. Liu and J. Li, *Appl. Surf. Sci.*, 255 (2009) 8629.
36. M. Deepa, T. K. Saxena, D. P. Singh, K. N. Sood and S. A. Agnihotry, *Electrochim. Acta*, 51 (2006) 1974.
37. M. Deepa, R. Sharma, A. Basu and S. A. Agnihotry, *Electrochim. Acta*, 50 (2005) 3545
38. B. G. Xie, J. J. Sun, Z. B. Lin and G. Nan. Chen, *J. Electrochem. Soc.*, 156 (2009) D79.
39. T.-Y. Kim, S. M. Cho, C. S. Ah, K. -S. Suh, H. Ryu and H. Y. Chu, *J. Inf. Display*, 15 (2014) 13.
40. B. Laik, D. Carrie`re and J. -M. Tarascon, *Electrochim. Acta*, 46 (2001) 2203.
41. P. C. Sunkanek, *J. Electrochem. Soc.*, 138 (1991) 1712.
42. R. Dewi, N. I. BaáYah and I. A. Talib, *Mater. Sci-Poland*, 25 (2007) 658.
43. Z. M. He, X. Yuan, Q. Wang, L. Yu, C. Zou, C. Y. Li, Y. Z. Zhao, B. F. He, L. Y. Zhang, H. Q. Zhang and H. Yang, *Adv. Optical Mater.*, 4 (2016) 106.
44. K. Shinozaki, *SID Digest*, 33 (2002) 39.
45. K. Bange, *Sol. Energ. Mat. Sol. C.*, 58 (1999) 1.
46. R. Viennet, J. P. Randin, I. D. Raistrick, *J. Electrochem. Soc.*, 129 (1982) 2451.
47. L. L. Yang, D. T. Ge, J. P. Zhao, Y. B. Ding, X. P. Kong and Y. Li, *Sol. Energ. Mat. Sol. C.*, 100 (2012) 251.
48. J. L. Zhou, G. Luo, Y. X. Wei, J. M. Zheng and C. Y. Xu, *Electrochim. Acta*, 186 (2015) 182.

49. A. Calleja, S. Ricart, M. Aklalouch, N. Mestres, T. Puig and X. Obradors, *J. Sol-Gel. Sci. Technol.*, 72 (2014) 21.
50. Utari, Kusumandari, B. Purnama and K. Abraha, *AIP Conference Proceedings*, 1755 (2016) 150018-1.

© 2017 The Authors. Published by ESG (www.electrochemsci.org). This article is an open access article distributed under the terms and conditions of the Creative Commons Attribution license (<http://creativecommons.org/licenses/by/4.0/>).